A&A 543, A13 (2012)
DOI: 10.1051/0004-6361/201219222

Astronomy & Astrophysics

Reddening and metallicity maps of the Milky Way bulge from VVV and 2MASS⋆

II. The complete high resolution extinction map and implications for Galactic bulge studies

O. A. Gonzalez[1], M. Rejkuba[1], M. Zoccali[2,3], E. Valenti[1], D. Minniti[2,4], M. Schultheis[5], R. Tobar[1], and B. Chen[5]

[1] European Southern Observatory, Karl-Schwarzschild-Strasse 2, 85748 Garching, Germany
e-mail: [ogonzale;mrejkuba;evalenti]@eso.org
[2] Departamento Astronomía y Astrofísica, Pontificia Universidad Católica de Chile, Av. Vicuña Mackenna 4860, Santiago, Chile
e-mail: [mzoccali;dante]@astro.puc.cl
[3] INAF – Osservatorio Astronomico di Bologna, via Ranzani, 40127 Bologna, Italy
[4] Vatican Observatory, V00120 Vatican City State, Italy
[5] Institut Utinam, CNRS UMR6213, OSU THETA, Université de Franche-Comté, 41bis avenue de l'Observatoire, 25000 Besançon, France

Received 14 March 2012 / Accepted 15 April 2012

ABSTRACT

Context. The Milky Way bulge is the nearest galactic bulge and the most readily accessible laboratory for studies of stellar populations in spheroids based on individual stellar abundances and kinematics. These studies are challenged by the strongly variable and often large extinction on a small spatial scale.
Aims. We use the Vista Variables in the Via Lactea (VVV) ESO public survey data to measure extinction values in the complete area of the Galactic bulge covered by the survey at high resolution.
Methods. We derive reddening values using the method described in Paper I. This is based on measuring the mean $(J - K_s)$ color of red clump giants in small subfields of $2' \times 2'$ to $6' \times 6'$ in the following bulge area: $-10.3^\circ \leq b \leq +5.1^\circ$ and $-10.0^\circ \leq l \leq +10.4^\circ$. To determine the reddening values $E(J - K_s)$ for each region, we measure the RC color and compare it to the $(J - K_s)$ color of RC stars measured in Baade's Window, for which we adopt $E(B - V) = 0.55$. This allows us to construct a reddening map sensitive to small-scale variations minimizing the problems arising from differential extinction.
Results. The significant reddening variations are clearly observed on spatial scales as small as $2'$. We find good agreement between our extinction measurements and Schlegel maps in the outer bulge, but, as already stated in the literature the Schlegel maps are unreliable for regions within $|b| \lesssim 6^\circ$. In the inner regions, we compare our results with maps derived from DENIS and *Spitzer* surveys. While we find good agreement with other studies in the corresponding overlapping regions, our extinction map is of higher quality owing to both its higher resolution and a more complete spatial coverage of the bulge. We investigate the importance of differential reddening and demonstrate the need for high spatial resolution extinction maps for detailed studies of bulge stellar populations and structure.
Conclusions. We present the first extinction map covering uniformly ∼315 sq. deg. of the Milky Way bulge at high spatial resolution. We consider a 30 arcmin window at a latitude of $b = -4^\circ$, which corresponds to a frequently studied low extinction window, the so-called Baade's Window, and find that its A_{K_s} values can vary by up to 0.1 mag. Larger extinction variations are observed at lower Galactic latitudes. The extinction variations on scales of up to $2'-6'$ must be taken into account when analyzing the stellar populations of the Galactic bulge.

Key words. Galaxy: bulge – dust, extinction – stars: abundances

1. Introduction

The Galactic bulge (GB) is one of the major components of the Galaxy and can be studied at a unique level of detail, in comparison to those of external galaxies, thanks to its proximity, which enables properties of individual stars to be measured. Bulge stars hold the imprints of how our Galaxy formed and evolved. The star formation and chemical enrichment history of the GB can be investigated in detail by analyzing the stellar ages and chemical abundances (McWilliam & Rich 1994; Zoccali et al. 2003; Fulbright et al. 2007; Rich et al. 2007; Lecureur et al. 2007; Zoccali et al. 2008; Clarkson et al. 2008; Brown et al. 2010; Bensby et al. 2010, 2011; Johnson et al. 2011; Gonzalez et al. 2011b).

Our current understanding of the Milky Way bulge structure and stellar content can be summarized as follows: i) the GB structure is dominated by the bar (Stanek et al. 1994), which appears to have a peanut or X-shape in the outer regions (McWilliam & Zoccali 2010; Nataf et al. 2010; Saito et al. 2011); ii) there is a radial stellar metallicity gradient (Zoccali et al. 2008; Johnson et al. 2011) that most likely flattens in the inner regions (Rich et al. 2007); iii) in addition to the population associated with the bar, there are hints of a second chemically and kinematically distinct component (Babusiaux et al. 2010; Hill et al. 2011; Gonzalez et al. 2011b; Bensby et al. 2011); and iv) the GB is dominated by old stars (Zoccali et al. 2003; Brown et al. 2010; Clarkson et al. 2011), although a younger population of metal-rich stars might be present as traced by microlensed dwarfs (Bensby et al. 2011). However, the general view of these properties, based on a more complete areal coverage, is expected

⋆ Based on observations taken within the ESO VISTA Public Survey VVV, Program ID 179.B-2002.

to provide a more complete picture of the Milky Way bulge formation history. Several projects designed to obtain this general view of the GB are either ongoing or planned for the near future (e.g. Minniti et al. 2010; Feltzing 2011; Ness & Freeman 2012; Elia Garcia Perez et al. 2012). The interpretation of these observations is inhibited by variations in the dust extinction properties on small scales towards the different GB regions.

The currently available extinction maps of the GB regions have different resolutions and coverages. The most commonly used extinction maps had been those of Burstein & Heiles (1982), until they were superseded by the Schlegel maps (Schlegel et al. 1998). The Schlegel extinction maps are full-sky maps of the dust color temperature based on IRAS and DIRBE experiments that are normalized to $E(B-V)$ values using a calibration of colors of background galaxies. Unfortunately, these maps suffer from large uncertainties in regions towards the GB. Specifically, as stated in Appendix C of Schlegel et al. (1998), the temperature structure of the Galaxy towards latitudes $|b| < 5°$ is not well-defined and contaminating sources have not been completely removed. Furthermore, as we show below, the resolution of these maps is too coarse. As a result, the Schlegel reddening values towards the GB are unreliable.

An extinction map covering $|b| < 5°$ of sufficiently high resolution to resolve the small spatial-scale variations in extinction, is important for an understanding of the general properties of the inner Galactic regions. Using red giant branch (RGB) stars from the near-IR photometric survey DENIS, Schultheis et al. (1999) provided a high resolution (2′) map in the inner regions of the GB ($|b| < 2°$). This map provides sufficient spatial resolution to permit analyses of these inner Galactic regions, but its coverage is too limited for a comprehensive study of the *global* GB stellar populations and structural properties.

More recently, Marshall et al. (2006) provided a full three-demensional (3D) extinction map of the GB. These 3D maps are indeed of high importance for Galactic studies towards the inner Galaxy as they hold the additional distance information. However, in order to build 3D extinction maps, a sufficient number of stars is required in each resolution element, which implies that only a modest resolution can be achieved. The method in Marshall et al. (2006) is based on a comparison of 2MASS photometry to the Besançon model. At low Galactic latitudes ($|b| < 3°$), 2MASS is strongly affected by incompleteness and blending due to a too low spatial resolution and high stellar density, limiting the ability to derive correct star counts and extinction. The resolution of Marshall's 3D extinction map is 15′, which is again too coarse to fully overcome the differential reddening problems at lower latitudes $|b| < 4°$.

Other important extinction maps are available with a partial coverage of the GB such as those of Kunder et al. (2008) and Sumi (2004). However, for detailed studies of the GB, a high resolution and homogeneous extinction map covering the complete area of interest is missing. The deep and near-IR photometry of the Vista Variables in the Via Lactea (VVV) ESO public survey of the GB (Minniti et al. 2010) provides the ideal dataset to create such a map. In Gonzalez et al. (2011c, Paper I) we showed an effective technique based on the color of red clump (RC) stars to trace the effects of extinction. In this article, we extend our analysis to the complete GB region covered by the survey and derive the first complete extinction map of the GB, using a homogeneous population, namely the red clump, at a resolution of 2′–6′ (Sect. 3). We compare our map to extinction maps in the literature in the corresponding overlap regions (Sect. 4), and we discuss the importance of high resolution extinction map in future GB studies (Sect. 5).

2. Determination of A_{K_s} values

2.1. VVV survey data

We use the ∼315 square degree coverage of the Galactic bulge from the VVV survey. This corresponds to the first data release (DR1) of the survey, as described in Saito et al. (2012). In Paper I, we presented a detailed description of a method used to produce the multiband (J, H, and K_s) catalogs required for our global study of the GB stellar populations. Thus, we now provide only a brief summary of the adopted procedure. Single-band catalogs for each VVV image, the so-called tiles, are produced at the Cambridge Astronomical Survey Unit (CASU). These catalogs are then individually calibrated to the 2MASS photometric system by comparing high quality stellar detections from both catalogs, in the magnitude range $12 < K_s < 13$ mag where both catalogs overlap. Sources brighter than $K_s = 12$ mag in each VVV tile are removed and replaced by 2MASS stellar detections, flagged with high quality photometry. This ensures the required photometric agreement between the 2MASS and VVV surveys and the correction of the catalogs for saturation at the bright end ($K_s < 12$). These single-band catalogs are then matched using STILTS (Taylor 2006) to produce our final multiband catalogs.

2.2. Mean color of the Galactic bulge red clump

Studies of the chemical abundances and age measurements of the GB towards Baade's Window, have shown that the GB is predominantly old (∼10 Gyr) (Ortolani et al. 1995; Zoccali et al. 2003; Brown et al. 2010; Clarkson et al. 2011) and that it shows a broad metallicity distribution with a peak near solar metallicity (McWilliam & Rich 1994; Zoccali et al. 2008; Johnson et al. 2011). Stellar evolutionary models can thus provide specific constraints on the expected intrinsic color of stars along the different evolutionary stages. The observed color can then be compared to that expected from models and its difference can be linked to an external factor, such as extinction. The metallicity of the GB is not spatially uniform, but it follows a gradient along its minor axis (Zoccali et al. 2008). Furthermore, the extent of these gradients towards other regions remains unclear. For this reason, uncertainties may prohibit the direct comparison of the observed red giant branch (RGB) stars' colors with those expected from models. Fortunately, this problem can be minimized by the use of RC giants, as the mean color of these stars has a small dependance on these parameters.

In Paper I, we used the multiband VVV catalogs to determine extinction values by measuring the mean $(J-K_s)$ color of the RC stars and comparing it to that of a region of known extinction, called Baade's Window. A selection box in the CMD of each tile is chosen to include only GB red clump stars. The limits of this box vary for each line of sight depending on the amount of extinction and were therefore inspected by eye and modified accordingly. A Gaussian fit to the $(J-K_s)$ color distribution is then used to determine the mean color of the red clump. For a $4′ \times 4′$ region in Baade's Window centered on coordinates $\alpha_{2000} = 18{:}04{:}51.2$ and $\delta_{2000} = -30{:}03{:}26.5$, the VVV photometry yields a $(J-K_s) = 0.96$ mag. Using the measured extinction of this field of $E(B-V) = 0.55 \pm 0.01$ mag (Sumi 2004; Kunder et al. 2008; Zoccali et al. 2008), we obtain a dereddened mean color of $(J-K_s)_0 = 0.68$ for the RC stars in this region. We use this value as a reference for the intrinsic mean color of the RC, and its difference with respect to the measured RC color in any other region is an indicator of the extinction, given by $E(J-K_s)$.

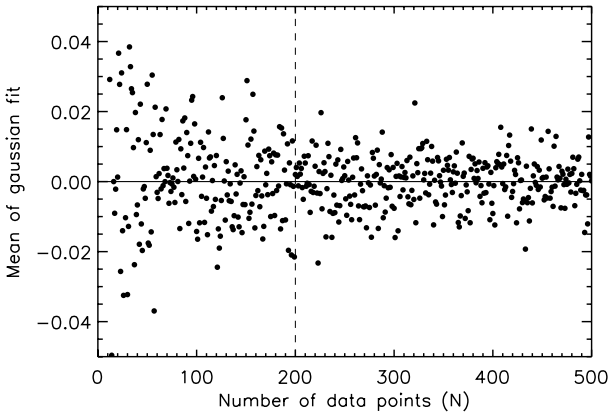

Fig. 1. The mean value obtained from a Gaussian fit to a set of N data points randomly distributed following a Gaussian distribution centered on zero (solid horizontal line) with a standard deviation of 0.10. The dashed vertical line shows the limit of 200 points adopted as the minimum number of stars in each subfield.

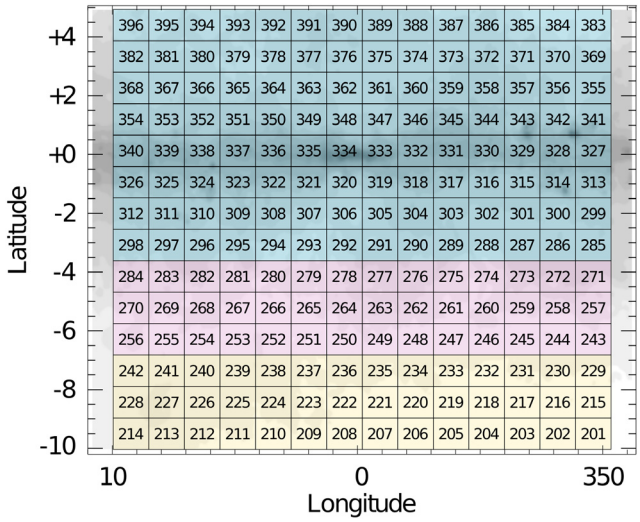

Fig. 2. VVV coverage of the GB in Galactic coordinates. Each small square shows the coverage by individual 1° × 1.5° tile from the VVV. Tile numbering for the VVV survey is described in Saito et al. (2012). The different color shading of the tiles depends on the spatial resolution (2′, 4′, and 6′, respectively) used to derive reddening from the mean color of the red clump stars (see text for details).

3. The complete high resolution extinction map

We computed the mean RC $(J - K_s)$ color in small subfields towards the complete GB region of VVV. We adapted the resolution to provide a sufficient number of RC stars (>200) to populate the color distribution and ensure sufficiently high quality, as well as minimize the effect of the differential extinction discussed in Paper I. The minimum number of 200 stars for each subfield was determined following the result shown in Fig. 1. The vertical axis of Fig. 1 shows the mean value obtained from a Gaussian fit to a set of N random values that follow a Gaussian distribution centered on zero that has a standard deviation of 0.10. The vertical dashed line shows the limit of 200 stars. The dispersion in the mean value from the Gaussian fits increases significantly for a number of data points below this limit. The resulting spatial resolution of the complete map depends on latitude, as shown in Fig. 2. For the latitude range $-3.5° \lesssim b \lesssim +5°$, the density of GB stars allowed the highest resolution of 2′ to be used. As the density of GB stars drops at greater distances from the plane, the resolution had to be reduced to 4′ for $-7° \lesssim b \lesssim -3.5°$ and to 6′ for $-10° \lesssim b \lesssim -7°$. The mean measured RC color is compared to the intrinsic value measured in Baade's Window to derive the reddening value $E(J - K_s)$. From $E(J - K_s)$, the A_{K_s} extinction values are obtained by applying a specific extinction law. Figure 3 shows the complete A_{K_s} extinction map for the GB VVV region based on the Cardelli et al. (1989) extinction law. The extinction variations in the inner 2° of the Galactic plane can be more clearly discerned in the upper panel of Fig. 6, where the highest values of extinction reach $A_{K_s} = 3.5$.

In a small number of regions, the differential reddening is too high even over 2′, resulting in large errors in the reddening measurements, or even in extreme cases preventing the identification of RC features. Some of these regions are visible as small white dots/squares in the upper panel of Fig. 6. They are less obvious in Fig. 3, because of the resampling in the innermost regions in the presentation of the figure. All of these regions are clearly identified as having large errors in our extinction database.

Our extinction maps clearly show small-scale variations, which are produced by the strong dust features traced, in particular at low latitudes. These features are now seen in great detail thanks to the high resolution and large coverage of our study.

3.1. A note about the extinction law

At present, there is no real consensus on which is the correct extinction law to be used for studies towards the inner GB. Each reddening map is related to a given extinction law that can vary between different studies. Recent results suggest that extinction properties might vary in different locations and possibly depend on the amount of extinction and dust properties. In particular, Nishiyama et al. (2006, 2008, 2009) presented a detailed study of the interstellar extinction law towards the inner regions of the GB ($|l| < 2°$, $|b| < 1.0°$), concluding that this varies significantly depending on the line of sight.

Nishiyama et al. (2006) also provided ratios of total to selective extinction that differ from the $R_V \sim 3.1$ standard extinction law obtained towards other regions.

The problem of the correct extinction law towards the GB is not adressed here, but will be part of another article (Chen et al., in prep.) based on GLIMPSE and VVV datasets. However, to obtain extinction values from the reddening map presented here, $E(J - K_s)$ values need to be transformed into an absolute extinction using a given extinction law. Here, we decided to adopt two different extinction laws. The first is the more commonly used extinction law from Cardelli et al. (1989). Adopting 1.240, 1.664, and 2.164 micron as the effective wavelengths of a K2 giant (typical of red clump stars) for 2MASS from Indebetouw et al. (2005), the coefficients corresponding to the Cardelli et al. (1989) extinction law are

$$A_J = 1.692E\,(J - K_s)\,, \quad (1)$$
$$A_H = 1.054E\,(J - K_s)\,, \quad (2)$$
$$A_{K_s} = 0.689E\,(J - K_s)\,. \quad (3)$$

The second is the extinction law from Nishiyama et al. (2009)

$$A_J = 1.526E\,(J - K_s)\,, \quad (4)$$
$$A_H = 0.855E\,(J - K_s)\,, \quad (5)$$
$$A_{K_s} = 0.528E\,(J - K_s)\,, \quad (6)$$

which was determined, for the 2MASS photometric system, in the inner regions of the GB closer to the Galactic plane.

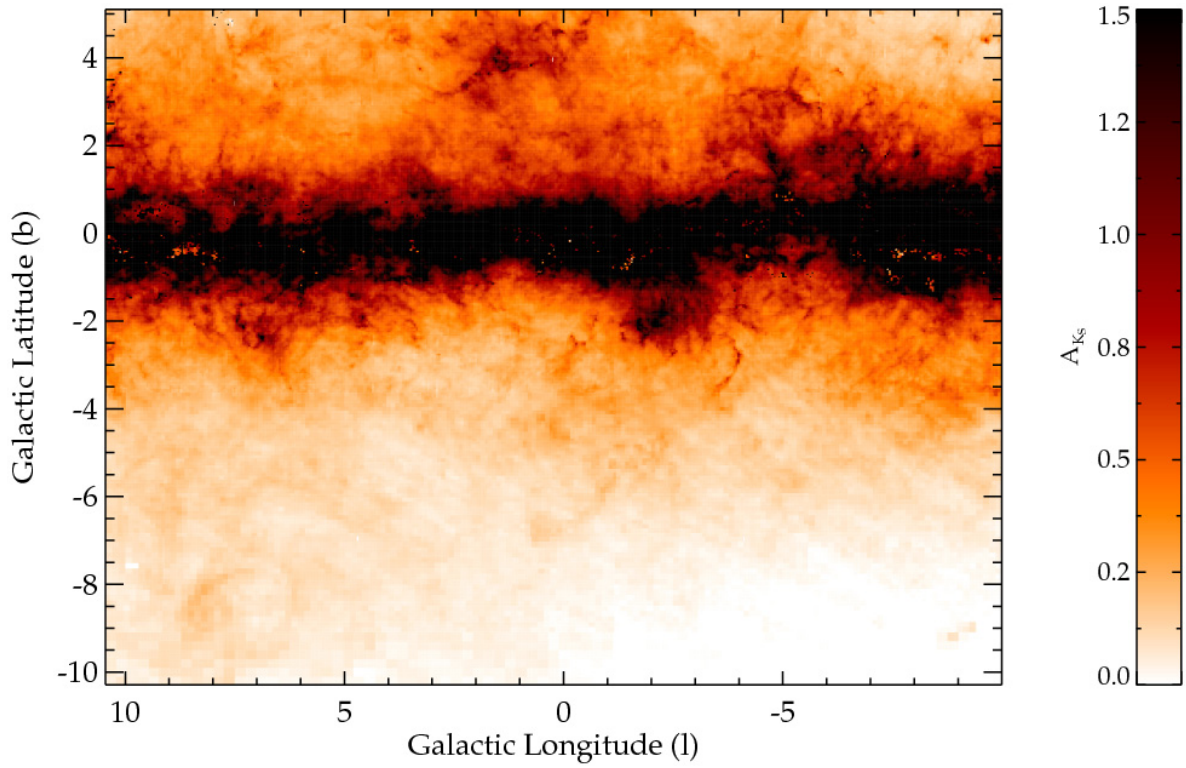

Fig. 3. Extinction map of the GB for the complete region covered by the VVV survey. The A_{K_s} values are computed from $E(J-K_s)$ measurements assuming Cardelli et al. (1989) extinction law for all tiles. At A_{K_s} values larger than 1.5 mag, the color scale saturates. The details of the extinction variation in the inner highly extincted regions, where A_{K_s} reaches up to 3.5 mag, can be more clearly seen in the upper panel of Fig. 6.

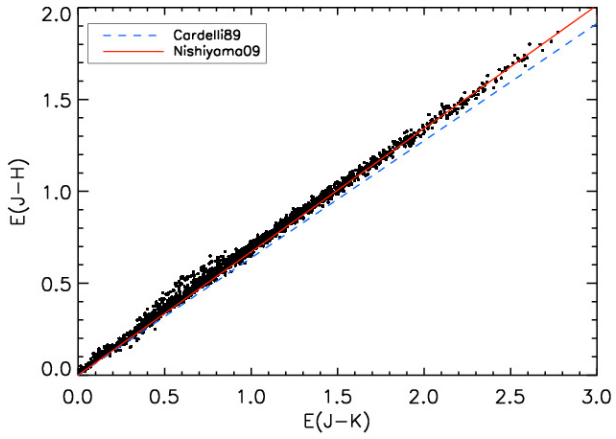

Fig. 4. $(J-K_s)$ and $(J-H)$ color difference between our control field and those measured in the subfields of tiles b317, b303, and b275. The size of the subfields corresponds to the same resolution described in Fig. 2. The blue dashed line shows the relation $E(J-H) = 0.638E(J-K_s)$ corresponding to the extinction law from Cardelli et al. (1989) and red solid line to $E(J-H) = 0.671E(J-K_s)$ from Nishiyama et al. (2009).

To determine the extinction that should be used, we performed the following exercise. We measured the colors $(J-K_s)$ and $(J-H)$ in our 4′ control field in Baade's window, where we found mean values of $(J-K_s) = 0.96$ and $(J-H) = 0.73$. We then measured these colors for a set of regions with different latitudes and compared them to those in our control field. The $E(J-K_s)$ and $E(J-H)$ color differences for each line of sight are shown in Fig. 4. The relation between these color differences can be obtained from the corresponding coefficients of each extinction law. Our measurements are in good agreement with those for the Nishiyama et al. (2009) extinction law, where $E(J-H) = 0.671E(J-K_s)$. However, since the implications discussed in Sect. 5 do not depend strongly on the adopted extinction law, we proceeded with our analysis following the more commonly used law of Cardelli et al. (1989).

3.2. BEAM calculator

As described in the following, our high-resolution extinction map of the GB provides a valuable tool for future studies. To make it available to the community, we developed a web-based tool called BEAM (Bulge Extinction And Metallicity) calculator[1]. This tool provides the user with an easy access to our measurements, both for the extinction values presented in this article, as well as for the photometric metallicities obtained in Paper I. The complete metallicity map and its analysis will be the subject of our upcoming Paper III (Gonzalez et al., in prep.).

The tool allows the user to input a set of coordinates and the corresponding size of the field of interest, retrieving the mean extinction (A_{K_s}) towards these set of coordinates. The extinction values are computed using either the Cardelli et al. (1989) or Nishiyama et al. (2009) extinction law. However, the $E(J-K_s)$ values are also always provided, so that the user can adopt any other extinction law of preference.

4. Comparison with existing extinction maps of the Galactic bulge

Other studies have addressed the problem of extinction towards the GB. Reddening maps providing a similar GB coverage as the one presented here are the 3D maps of Marshall et al. (2006) and the Schlegel et al. (1998) maps. As described in

[1] http://mill.astro.puc.cl/BEAM/calculator.php

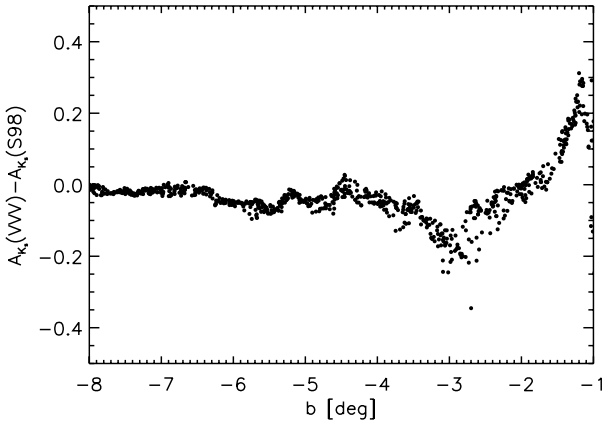

Fig. 5. Difference between the A_{K_s} values obtained in this work and those of Schlegel et al. (1998), as a function of Galactic latitude, for 1000 randomly distributed 30′ × 30′ regions between ($-8° < b < -1°$).

the introduction, it is well-known that the Schlegel maps cannot be trusted for regions closer to the Galactic plane ($|b| < 5°$) owing to contaminating sources and uncertainties in the dust temperatures. To quatify these effects, we compared our extinction values to a set of lines of sight at different latitudes. We retrieved A_V values from the Schlegel maps for 1000 regions of 30′ × 30′ size, randomly distributed across latitudes of $-8° < b < -1°$ for $0° < l < 2°$. Although the relative difference between the A_{K_s} values in Schlegel maps and ours will not depend on the adopted extinction law, we converted their A_V values to A_{K_s} following the Cardelli et al. (1989) law and then retrieved our own A_{K_s} values from the BEAM calculator for the same target fields, again selecting the Cardelli et al. (1989) extinction law. Figure 5 shows the comparison between our extinction results and those of Schlegel et al. (1998) as a function of latitude. The difference its already visible at $b < -6°$ and becomes much larger for latitudes closer to the plane. Interestingly, we observe that there is a negative difference between our A_{K_s} values and those of Schlegel et al. (1998) for $b < -2°$, while this difference is positive at $b > -2°$. The source of this sign variation is not obvious given the uncertainties in the Schlegel maps at those latitudes.

Marshall et al. (2006) provided an extinction map for the complete GB, obtained by comparing the 2MASS photometry to the Besançon model, including the model-dependent extinction as a function of distance along each line of sight. Unfortunately, this technique only allows us to calculate the maps with a lower resolution (15′), which is insufficient to resolve the small-scale extinction variations in the inner GB regions.

The studies of Schultheis et al. (1999, 2009) provided very high resolution maps (2′), which were obtained using DENIS and *Spitzer* data respectively for the inner $|b| < 2°$. Since in these regions the small-scale extinction variations are particularly strong, these datasets are ideal for comparison with our extinction maps and study possible systematics between the methods. The *Spitzer* map of Schultheis et al. (2009) covers specifically the central ∼1° regions of the Galaxy. This region is also included in the DENIS map and the extinctions derived from DENIS and *Spitzer* observations agree very well.

To produce the DENIS extinction maps, Schultheis et al. (1999) used a method based on comparison of GB RGB colors in 2′ subfields with model isochrones from Bertelli et al. (1994). They adopted a solar metallicity population at a distance of 8 kpc with an age of 10 Gyr in the model isochrones. The same process was adopted to produce the *Spitzer* extinction maps of Schultheis et al. (2009). This method has the benefit of using bright GB stars, thus minimizing problems arising from photometric errors and (in-)completeness. However, the colors of RGB stars are much more strongly affected by population effects, in particular metallicity and to a lesser extent age, when compared to RC stars in our method. The colors of RGB stars are frequently used to derive the metallicity distribution function of stellar populations when the spectroscopy of individual stars is unavailable.

The influence of population effects on the RC magnitudes and color has been investigated both theoretically (Girardi & Salaris 2001; Salaris & Girardi 2002) and observationally (Alves 2000; Grocholski & Sarajedini 2002; Pietrzyński et al. 2003; Laney et al. 2012). In both cases, RC stars appear to provide a reliable standard distance indicator, considering the possible variations in the general GB population properties. If we were to consider a variation in the mean GB metallicity to go from solar down to [Fe/H] = −0.4, as obtained from the spectroscopic metallicity distributions of Zoccali et al. (2008), we would expect an error in the mean RC color of ∼0.08 mag, which is equivalent to a variation of $A_{K_s} = 0.06$ mag assuming the Cardelli et al. (1989) extinction law and $A_{K_s} = 0.04$ mag for a Nishiyama et al. (2009) law.

The extinction maps of Schultheis et al. (1999), based on the magnitudes of RGB and AGB stars, were produced at latitudes $b < 2°$ where no or only a very weak metallicity gradient seems to be present (Rich et al. 2007). Thus, extinctions obtained from an isochrone comparison to red giant stars should be reliable for the regions studied by Schultheis et al. (1999), and their errors should be dominated by the distance uncertainty of the RGB population along each line of sight. However, this method would have a considerable problem when used to construct a global extinction map, such us the one presented here.

Figure 6 compares our extinction map with that of Schultheis et al. (1999) using DENIS photometry. The A_V values of Schultheis et al. (1999) were converted to A_{K_s} following the extinction law of Cardelli et al. (1989) for comparison purposes. Their similarity is remarkable, with both maps tracing the same dust concentrations in the inner regions. We can also directly compare the extinction values retrieved from the BEAM calculator to those of Schultheis et al. (1999) and Schultheis et al. (2009). This comparison is shown in Fig. 7. The A_{K_s} values of both methods are in good agreement with a scatter on the order of 0.2 mag, which is expected from the different methods and photometric errors. The scatter becomes larger, up to 0.6 mag, in the regions of higher extinction ($A_{K_s} > 2$), where for a significant number of lines of sight we find a lower extinction value than Schultheis et al. (2009). A possible explanation for this difference is that, in these highly reddened regions, the extinction is enough to bring RC stars to magnitudes fainter than $K_s \sim 17$, where the completness of VVV is on the order of 60% (Saito et al. 2012) and therefore our reddening values might have been underestimated. However, we emphasize that this difference is observed in the inner 1° × 1° of the GB where extinction determinations are certainly more complicated. Moreover, the overall agreement is remarkable considering the different techniques, data sets, and stellar populations (RC vs. RGB) of our studies.

5. Implications for Galactic bulge studies

Extinction corrections are fundamental to essentially all studies of stellar populations, as well as for the measurements of

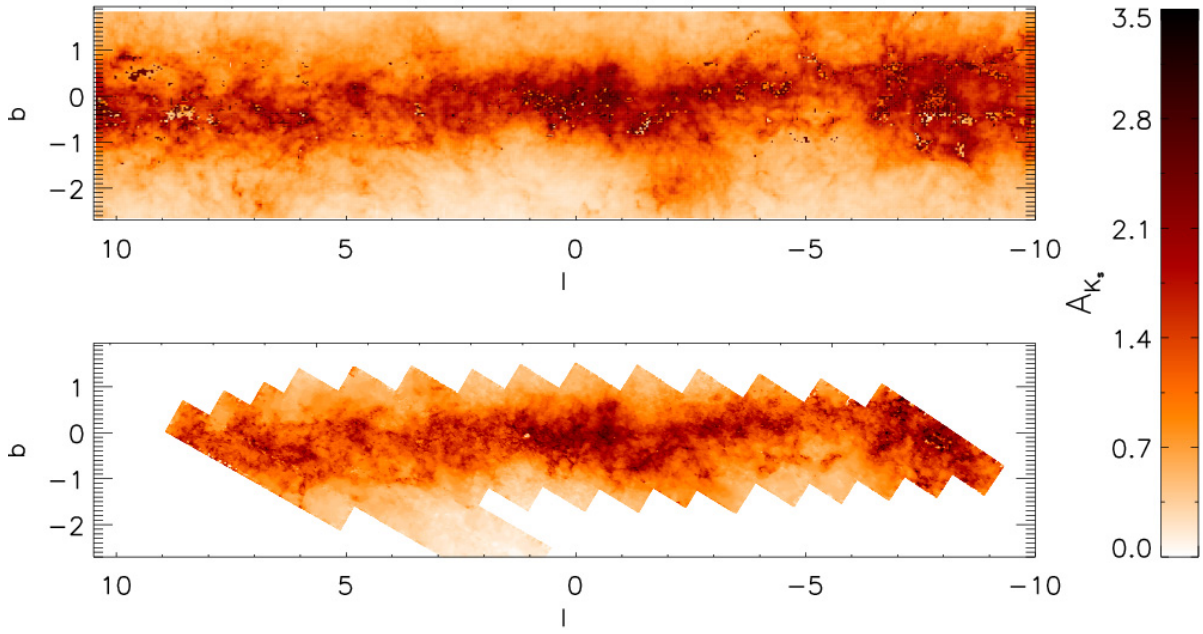

Fig. 6. The upper panel shows the inner ∼4° region around the Galactic plane of our VVV extinction map. The A_{K_s} values are based on the Cardelli et al. (1989) extinction law. Part of this region was also covered by the DENIS survey, which was used in Schultheis et al. (1999) to build the extinction map shown in the lower panel.

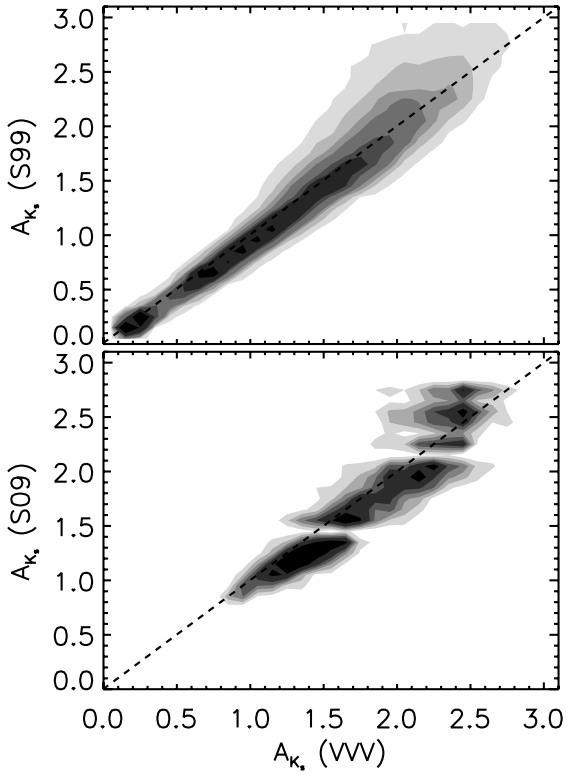

Fig. 7. *Upper panel* shows the comparison of the A_{K_s} values obtained in this work and those of Schultheis et al. (1999) for the common inner Bulge region ($-2° < b < +2°$). *Lower panel* shows the comparison with the *Spitzer* extinction map of Schultheis et al. (2009) for the central 1° of the Galaxy. Both plots are shown as density contours due to huge number of data points.

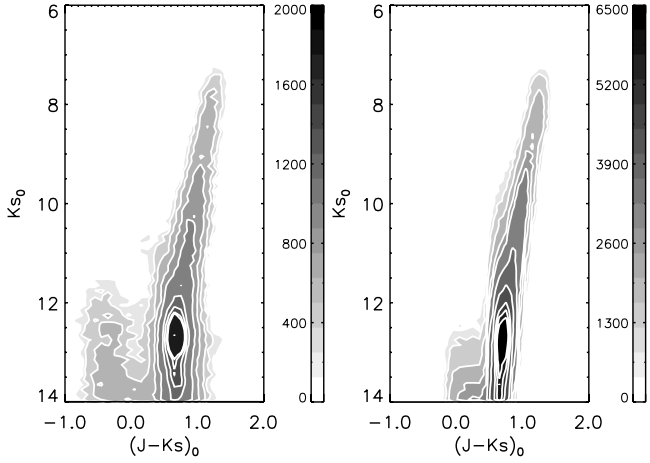

Fig. 8. *Left panel* shows HESS diagram of a 40′ region in the inner Bulge $(l, b) = (-1.0, -1.0)$. The *right panel* shows the diagram for the same region as obtained from the Besancon model.

distances and structural parameters. In this section, we highlight the advantages provided by our new high-resolution and large-area extinction map for studies of color-magnitude diagrams, determinations of stellar parameters in spectroscopic abundance studies, and both distance and structural studies of the GB.

5.1. The color-magnitude diagram of the inner Galactic bulge

The VVV color-magnitude diagrams are de-reddened using our new extinction map of the GB. In Fig. 8, we compare the observed, extinction-corrected, inner GB CMD with the predictions of the population synthesis model of the Milky Way from the Besançon group including the thin disk, thick disk, and bulge populations. This model is described in detail in Robin et al. (2012). It uses the Marshall et al. (2006) extinction map and when compared with the observations, such as 2MASS star counts, can be used to study the structure of the Milky Way. As already mentioned above, in the innermost regions of the GB, 2MASS is severely incomplete and affected by strong crowding and blending, which thus limit the predictive power of the model

in the inner regions. With the superior spatial resolution of the VVV survey (median seeing is better than 0.9″ in J, H, and K_s images) and its deeper photometry, it is now possible to make direct comparisons with the simulations and thus validate some of the assumptions adopted in the model.

Figure 8 shows a Hess diagram of a 40′ × 40′ region centered on the Galactic coordinates $(l, b) = (1.0°, -1.0°)$ (VVV tile b320) in the left panel. In the right panel, we present the CMD obtained from the Besançon model for the same region. There is a remarkable similarity between our dereddened data and the model. A major difference is found for the blue plume of stars at $(J - K_s)_0 \sim -0.2$ in the left diagram, which is much stronger, brighter, and bluer in the VVV CMD than the blue sequence at $(J - K_s)_0 \sim 0.1$ in the model. This part of the CMD contains the disk stars, which are all found along the line of sight towards the GB, hence have a range of reddening values, some having significantly lower reddening than derived for the GB red clump stars. After applying the extinction correction appropriate for the GB stars, the colors of the disk stars cannot be therefore correctly reproduced in our CMDs, even though the colors and magnitudes of the major GB features, the RC, and the RGB are all in excellent agreement with the model. This provides evidence that VVV dereddened color-magnitude diagrams can be used to investigate the stellar population properties, such as age and metallicity distributions of stars even in the inner GB regions. In addition, the good agreement between the model and the observations indicates that we could compare the Besançon model to observed VVV data, in order to obtain 3D extinction maps such as the one from Marshall et al. (2006). The high spatial resolution and photometric depth of VVV CMDs offer the possibility to derive the 3D extinction map of the GB with a resolution of up to 6′ for the inner regions (Chen et al., in prep.). Although this resolution, which is limited by the number of stars required for the comparison, is lower than that of the map presented here, it will add important 3D information, allowing a more accurate characterization of the structure in the inner GB.

5.2. Photometric effective temperatures

Low- and intermediate-resolution spectroscopic studies, where the determination of the stellar parameters is based on the photometric properties of the targets, depend on the adopted extinction corrections. In particular, the critical parameter is the effective temperature that is derived from the color of the stars. Current studies of the GB use multi-object fibre spectrographs with large fields of view in order to observe simultaneously large numbers of targets. The field of view can range from the 25′ radius for the FLAMES spectrograph on the VLT (Pasquini et al. 2003) to the 2° field of the AAOmega multifibre spectrograph at the AAT (Sharp et al. 2006). Assuming that a single value of extinction is adopted for a single pointing, using our 2′ resolution extinction map we can estimate the differential extinction in a typical region of say 30′ and derive the effect on the corresponding effective temperatures determined from colors of stars.

The relative effect of differential reddening does not depend significantly on the adopted calibration, and in our experiment we use the photometric calibration of Ramirez & Melendez (2005) for giant stars. A typical GB K giant star has solar metallicity and an effective temperature of around 4500 K. According to the calibration of Ramírez & Meléndez (2005), this star will have an intrinsic color of $(V - K_s)_0 = 2.625$. We now consider a 30′ region located at a latitude of $b = -4°$ along the minor axis ($l = 0°$) and retrieve the extinction values using our BEAM calculator for a set of 200 randomly distributed positions within this region. These individual extinctions differ from the mean extinction for the whole region depending on the amount of the differential extinction. If we add this difference to the intrinsic color of the star and use the new color to calculate the corresponding effective temperature from the photometric calibration, we can estimate the effect of differential reddening when adopting a single reddening value for the whole region. The difference between the original effective temperature and the one obtained after including the effect of differential extinction is shown in Fig. 9 as a function of the variation in A_{K_s}. The amount of extinction A_{K_s} varies by 0.10 mag in the 30′ region, which produces an error of up to 300 K in effective temperature. This effect becomes even more important in regions of higher extinction than Baade's Window as shown for the case of latitude $b = -2°$ (red circles in Fig. 9). Here a 0.30 mag extinction variation is observed within the 30′ region, which leads to errors that are even larger than 600 K in the derived photometric effective temperature.

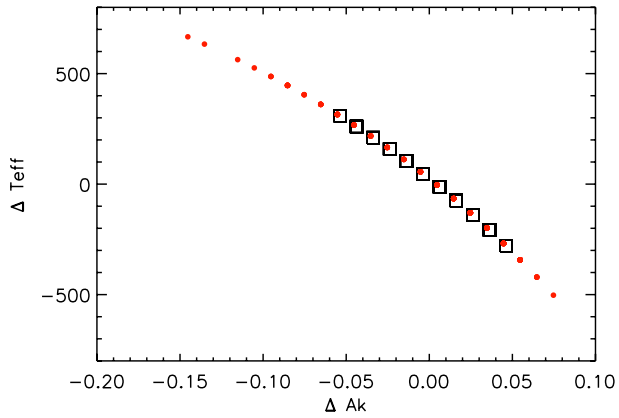

Fig. 9. The effect of differential reddening towards the Bulge for the determination of photometric effective temperatures. We plot the variations in the A_{K_s} values for a set of 200 random positions in a 30′ region towards $b = -4°$ (black squares) and $b = -2°$ (red circles), as obtained from the BEAM calculator, and compare them to variations in the photometric effective temperature.

All studies relying on photometric determination of the effective temperature clearly need to take into account these extinction variations and correct for them. The strong differential reddening in the inner Galaxy may otherwise result in large errors in the abundance measurements. While the dependence of metallicity error on temperature is not necessarily linear, and depends on the spectral type of the target, for reference we recall that an error of 200 K in effective temperature led to a measurement error in [Fe/H] of 0.1 dex for K giant stars in the GB (Zoccali et al. 2008).

5.3. Distances and the Galactic bulge structure

As shown in Gonzalez et al. (2011c), the dereddened magnitudes of the VVV survey can be used to build the GB luminosity function towards different lines of sight, thus measure the mean magnitude of the RC and derive the mean distance to different regions of the GB. This technique has been used in several studies to study the orientation angle of the Galactic bar (Stanek et al. 1997; Rattenbury et al. 2007; Cabrera-Lavers et al. 2007) and the X-shape morphology of the outer GB regions (Saito et al. 2011).

In Gonzalez et al. (2011a), we studied the bar orientation in the inner regions ($b = \pm 1°$) by measuring the mean RC magnitudes as a function of longitude. Using the homogeneous

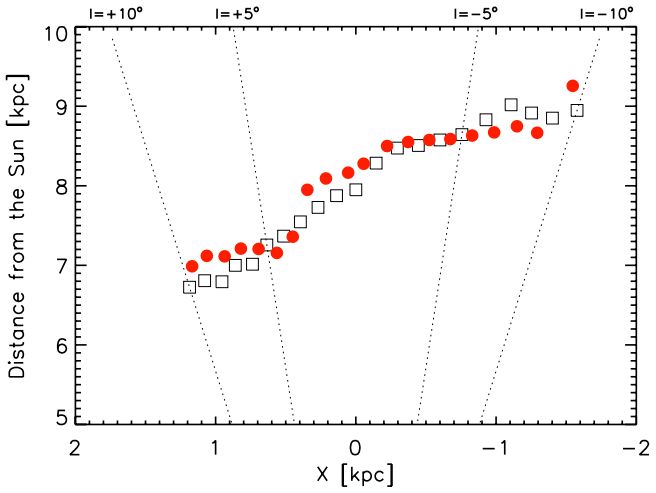

Fig. 10. Position of the Galactic bar with respect to the Sun as measured with the RC method from the the dereddened K_s magnitudes using our extinction map (red filled circles) at a latitude of $b = -5°$. Also shown, are the measurements from the Galactic model as presented in Gerhard & Martinez-Valpuesta (2012) at the same latitude, corresponding to a bar with an angle of 25° with respect to the Sun-Galactic center line of sight (black empty squares). Dotted lines mark the lines of sight for longitudes $l = \pm 5°$ and $l = \pm 10°$.

extinction map presented here, this study can now be extended to other regions of the GB. These measurements should ideally be compared to a galactic model similar to that of Martinez-Valpuesta et al. (2006). Interestingly, although this model has not been fine-tuned in any way to reproduce the properties of the Milky Way, in Gerhard & Martinez-Valpuesta (2012) the model was shown to nicely reproduce the observed structural properties of the GB, including the change in the bar inclination in the inner regions, as measured by Nishiyama et al. (2005) and Gonzalez et al. (2011a). This model also provides predictions for higher latitudes, which can now be validated using our extinction-free magnitudes. Figure 10 shows the position of the bar with respect to the Sun as measured from the mean dereddened K_s VVV magntiudes and the model of Gerhard & Martinez-Valpuesta (2012) at higher Galactic latitude $b = -5°$. The agreement between our observations and the model is remarkable, confirming that the Milky Way bar is inclined at 25 deg with respect to the Sun-Galactic center line of sight. The correction for differential extinction provided by our new map allows us to extend this comparison of the model and observations to the complete GB, including the characterization of the stellar density profile, the observed X-shape, and other structural indicators.

6. Conclusions

We have used the VVV dataset to produce a high-resolution extinction map of the GB covering the approximately 315 square-degree area of $-10.3° \leq b \leq +5.1°$ and $-10.0° \leq l \leq +10.4°$. We used the color of RC stars to trace the effect of extinction in the subfields of $2' \times 2'$ for $-3.5° \lesssim b \lesssim +5°$, $4' \times 4'$ for $-7° \lesssim b \lesssim -3.5°$, and $6' \times 6'$ for $-10° \lesssim b \lesssim -7°$, providing a first reddening map sensitive to the small-scale variations that homogeneously covers the whole GB.

An excellent agreement is found when comparing the common regions of our full VVV map with those of DENIS (Schultheis et al. 1999) and *Spitzer* maps (Schultheis et al. 2009), which cover the very inner regions of the GB ($|b| < 2°$). We have also compared our maps with those of Schlegel et al. (1998) at different latitudes and confirm that the Schlegel maps should not be used for latitudes $|b| < 5°$ towards the Milky Way bulge.

The reddening map presented here is particularly useful when the global picture of the GB is investigated. We have presented some of the direct consequences of using a higher resolution map, when studying both the stellar populations and the structure of the GB. We have shown that a typical 30′ region at $b = -4°$, for which a single extinction value is normally assumed, has a variation due to differential reddening of up to 0.10 mag. This effect is even larger in the inner regions where differential reddening produces variations of more than 0.35 mag in a similar field size. This has a strong impact on stellar population properties derived from the color of stars, such as the photometric effective temperature. We show that errors of more than 500 K can be caused by differential extinction in a 30′ region if a single extinction value is adopted. The current map allows us to avoid these errors. In addition, we show that the observed CMD of an inner GB region at $(l, b) = (1.0, -1.0)$ closely matches a CMD produced using the Besançon stellar population model where the effects of extinction are obviously not present.

We have shown how the combination of a good treatment of extinction and a dataset similar to that presented here, provides the ideal tool for the study of the inner Galactic structure based on the luminosity function properties. We used the VVV data to measure the mean RC magnitude of the GB towards different longitudes at $b = -5°$, following the method described in (Gonzalez et al. 2011b). We found a remarkable agreement between our measurements and those of the model of Martinez-Valpuesta et al. (2006) for a bar at 25° with respect to the Sun-Galactic center line of sight. Gerhard & Martinez-Valpuesta (2012) demonstrated how the model reproduces our observations in the inner GB ($b = \pm 1°$) and we have shown here that this is also true at higher latitudes. With our full extinction map, it is possible to compare the global GB structure to models such as that of Martinez-Valpuesta et al. (2006).

Our extinction map is available to the community via a web-based tool BEAM (Bulge Extinction And Metallicity) calculator. The complete photometric metallicity map (Gonzalez et al., in prep.) will also be available from the same site. These maps are an important step towards improving our understanding of the general properties of the Galactic bulge and will be a particularly valuable tool for upcoming spectroscopic surveys of the inner Galaxy.

Acknowledgements. We thank Pascal Fouqué for important suggestions about this work. We acknowledge the anonymous referee for helpful comments on this article. We gratefully acknowledge use of data from the ESO Public Survey program ID 179.B-2002 taken with the VISTA telescope, and data products from the Cambridge Astronomical Survey Unit. We acknowledge funding from the FONDAP Center for Astrophysics 15010003, the BASAL CATA Center for Astrophysics and Associated Technologies PFB-06, the MILENIO Milky Way Millennium Nucleus from the Ministry of Economycs ICM grant P07-021-F, and Proyectos FONDECYT Regular 1110393 and 1090213. M.Z. acknowledges a fellowship from the John Simon Guggenheim Memorial Foundation. M.Z. is also partially supported by Proyecto Anillo ACT-86. This publication has made use of data products from the Two Micron All Sky Survey, which is a joint project of the University of Massachusetts and Infrared Processing and Analysis Center/California Institute of Technology, funded by the National Aeronautics and Space Administration and the National Science Foundation. We warmly thank the ESO Paranal Observatory staff for performing the observations.

References

Alves, D. R. 2000, ApJ, 539, 732
Babusiaux, C., Gómez, A., Hill, V., et al. 2010, A&A, 519, A77
Bensby, T., Feltzing, S., Johnson, J. A., et al. 2010, A&A, 512, A41
Bensby, T., Adén, D., Meléndez, J., et al. 2011, A&A, 533, A134

Bertelli, G., Bressan, A., Chiosi, C., Fagotto, F., & Nasi, E. 1994, A&AS, 106, 275
Brown, T. M., Sahu, K., Anderson, J., et al. 2010, ApJ, 725, L19
Burstein, D., & Heiles, C. 1982, AJ, 87, 1165
Cabrera-Lavers, A., Hammersley, P. L., González-Fernández, C., et al. 2007, A&A, 465, 825
Cardelli, J. A., Clayton, G. C., & Mathis, J. S. 1989, ApJ, 345, 245
Clarkson, W., Sahu, K., Anderson, J., et al. 2008, ApJ, 684, 1110
Clarkson, W. I., Sahu, K. C., Anderson, J., et al. 2011, ApJ, 735, 37
Elia Garcia Perez, A., Allende Prieto, C., Bizyaev, D., et al. 2012, in American Astronomical Society Meeting Abstracts, 219, 410.04
Feltzing, S. 2011, in Stellar Clusters & Associations: A RIA Workshop on Gaia, 311
Fulbright, J. P., McWilliam, A., & Rich, R. M. 2007, ApJ, 661, 1152
Gerhard, O., & Martinez-Valpuesta, I. 2012, ApJ, 744, L8
Girardi, L., & Salaris, M. 2001, MNRAS, 323, 109
Gonzalez, O. A., Rejkuba, M., Minniti, D., et al. 2011a, A&A, 534, L14
Gonzalez, O. A., Rejkuba, M., Zoccali, M., et al. 2011b, A&A, 530, A54
Gonzalez, O. A., Rejkuba, M., Zoccali, M., Valenti, E., & Minniti, D. 2011c, A&A, 534, A3
Grocholski, A. J., & Sarajedini, A. 2002, AJ, 123, 1603
Hill, V., Lecureur, A., Gómez, A., et al. 2011, A&A, 534, A80
Indebetouw, R., Mathis, J. S., Babler, B. L., et al. 2005, ApJ, 619, 931
Johnson, C. I., Rich, R. M., Fulbright, J. P., Valenti, E., & McWilliam, A. 2011, ApJ, 732, 108
Kunder, A., Popowski, P., Cook, K. H., & Chaboyer, B. 2008, AJ, 135, 631
Laney, C. D., Joner, M. D., & Pietrzyński, G. 2012, MNRAS, 419, 1637
Lecureur, A., Hill, V., Zoccali, M., et al. 2007, A&A, 465, 799
Marshall, D. J., Robin, A. C., Reylé, C., Schultheis, M., & Picaud, S. 2006, A&A, 453, 635
Martinez-Valpuesta, I., Shlosman, I., & Heller, C. 2006, ApJ, 637, 214
McWilliam, A., & Rich, R. M. 1994, ApJS, 91, 749
McWilliam, A., & Zoccali, M. 2010, ApJ, 724, 1491
Minniti, D., Lucas, P. W., Emerson, J. P., et al. 2010, New Astron., 15, 433
Nataf, D. M., Udalski, A., Gould, A., Fouqué, P., & Stanek, K. Z. 2010, ApJ, 721, L28
Ness, M., & Freeman, K. 2012, Assembling the Puzzle of the Milky Way, Le Grand-Bornand, France, ed. C. Reylé, A. Robin, & M. Schultheis, EPJ Web Conf., 19, 6003
Nishiyama, S., Nagata, T., Baba, D., et al. 2005, ApJ, 621, L105
Nishiyama, S., Nagata, T., Kusakabe, N., et al. 2006, ApJ, 638, 839
Nishiyama, S., Nagata, T., Tamura, M., et al. 2008, ApJ, 680, 1174
Nishiyama, S., Tamura, M., Hatano, H., et al. 2009, ApJ, 696, 1407
Ortolani, S., Renzini, A., Gilmozzi, R., et al. 1995, Nature, 377, 701
Pasquini, L., Alonso, J., Avila, G., et al. 2003, in SPIE Conf. 4841, ed. M. Iye, & A. F. M. Moorwood, 1682
Pietrzyński, G., Gieren, W., & Udalski, A. 2003, AJ, 125, 2494
Ramírez, I., & Meléndez, J. 2005, ApJ, 626, 446
Rattenbury, N. J., Mao, S., Sumi, T., & Smith, M. C. 2007, MNRAS, 378, 1064
Rich, R. M., Origlia, L., & Valenti, E. 2007, ApJ, 665, L119
Robin, A. C., Marshall, D. J., Schultheis, M., & Reylé, C. 2012, A&A, 538, A106
Saito, R. K., Zoccali, M., McWilliam, A., et al. 2011, AJ, 142, 76
Saito, R. K., Hempel, M., Minniti, D., et al. 2012, A&A, 537, A107
Salaris, M., & Girardi, L. 2002, MNRAS, 337, 332
Schlegel, D. J., Finkbeiner, D. P., & Davis, M. 1998, ApJ, 500, 525
Schultheis, M., Ganesh, S., Simon, G., et al. 1999, A&A, 349, L69
Schultheis, M., Sellgren, K., Ramírez, S., et al. 2009, A&A, 495, 157
Sharp, R., Saunders, W., Smith, G., et al. 2006, in SPIE Conf. Ser., 6269
Stanek, K. Z., Mateo, M., Udalski, A., et al. 1994, ApJ, 429, L73
Stanek, K. Z., Udalski, A., Szymanski, M., et al. 1997, ApJ, 477, 163
Sumi, T. 2004, MNRAS, 349, 193
Taylor, M. B. 2006, in Astronomical Data Analysis Software and Systems XV, ed. C. Gabriel, C. Arviset, D. Ponz, & S. Enrique, ASP Conf. Ser., 351, 666
Zoccali, M., Renzini, A., Ortolani, S., et al. 2003, A&A, 399, 931
Zoccali, M., Hill, V., Lecureur, A., et al. 2008, A&A, 486, 177